International Journal of Research Publication and Reviews

Journal homepage: www.ijrpr.com ISSN 2582-7421

Design and Development of an Efficient Controller for DC-DC Boost Converter

Dr. J.S.V. Siva Kumar[a], M. Varun Kumar[b], P. Sai Teja[b], S. Akash[b], M.V.S, Karthik[b], P. Vasanth Kumar[b], P.S.J. Naidu[b]

[a]*Associate Professor, GMR Institute of Technology, Rajam, Andhra Pradesh, India*
[b]*UG Student, GMR Institute of Technology, Rajam, Andhra Pradesh, India*

A B S T R A C T

The purpose of this research is on using the state-space average technique to simulate a DC-DC boost converter having an unknown resistive nature load and an external input voltage, with the goal of developing an effective controller for this type of converter. The state-space average approach will be used for this work. The design of this controller will make use of the state-space average technique. To make the converter's control system, an analogous circuit modelling–based control method is adopted. The evolution of the adjusting regulations was facilitated by the use of state observers as a data source. This paper demonstrates that a closed loop system with a sliding mode controller and a boost converter can operate asymptotically stable. Adaptive controller robustness against input voltage and load parameter uncertainty and changes is evaluated experimentally. The findings of these experiments are included into the design process moving forward. Modelling and constructing the control scheme was followed by an investigation of the control scheme's performance and reactions using MATLAB/Simulink.

Keywords:DC-DC converter, Robustness, State space averaging, Sliding mode control

1. Introduction

Worldwide reliance on petroleum as a fuel source for vehicles is a major contributor to the rapid depletion of petroleum reserves. Greenhouse gas emissions, which are bad for people and the planet, have been rising steadily due in large part to this. Therefore, there has been a rise of interest in creating vehicles that run on nonconventional fuels. Thus, the increasing demand for EVs over the past two decades can be attributed to the automobile industry's focus on alternative propulsion technologies. Automakers have demonstrated more interest in Hybrid Electric Vehicles than in pure Electric Vehicles (HEV). Since the first hybrid car was introduced in 1900 by the Lohner Coach Factory; this vehicle had a hub motor powered by a generator coupled to a gasoline engine and a small battery for backup. However, advancements in ICE technology and falling oil prices have made ICE-powered vehicles more appealing than HEVs in recent years. Consequently, advancements in HEV technology halted until the last two decades, when the price of petroleum began to climb due to its scarcity and increased consumption, as well as because of the deteriorating atmospheric and environmental conditions produced by pollutants from hydrocarbon burning. Hybrid electric vehicles (HEVs) use electrical energy storage in addition to the internal combustion engine (ICE) to provide traction power, unlike traditional vehicles, which rely solely on the ICE. As a result, the vehicle's energy conversion can be improved, leading to greater efficiency, greater manoeuvrability, and fewer pollutants. What's more, the vehicle's electrical storage system can be regenerated during braking, further enhancing the system's efficiency.

Improving the performance of the controller utilised in the HEV drive train's power converter—which might be a boost converter, a buck converter, a buck-boost converter, or even a bidirectional converter — is a major design goal. The converter's output voltage will be regulated by the controller based on the current load. There will be instances when greater power is needed to propel the burden. It is possible to increase the voltage output of an Energy Storage System by increasing the number of cells included within its battery pack (ESS). However, increasing the voltage also has the unintended side effect of making the system bulkier, more expensive, and less practical for use in cars. Therefore, a Bi-directional DC-DC Boost converter might be used in HEVs to circumvent this issue. The current and consequent losses can be minimised by using a bidirectional DC-DC boost converter to increase the ESS voltage to the needed higher level. The bidirectional DC-DC converter's ability to allow power to flow back to the ESS during regenerative braking is another way in which it improves efficiency. The Bidirectional DC-DC converter's improved efficiency and regenerative energy capabilities make it a more attractive choice for power conversion in the HEV drivetrain, which in turn reduces the system's overall cost, size, and weight.

2. DC-DC Boost Converter

The term "DC-DC boost converter" is used to describe a certain type of DC-DC converter that has a higher output than input. This type of DC-DC converter is sometimes known as a "step-up DC-DC converter" since it boosts the input voltage. In dc-dc boost architectures, which increase the voltage of dc circuits, the input energy is temporarily stored before being released into the outcome at a greater voltage. Both magnetic and electric field storage elements can be used to store data utilising a wide range of active and passive switching mechanisms. The PWM boost converter requires only three components to increase the dc voltage. Power field-effect transistors (FETs) were first developed in the late 1980s and allow for higher frequency operation with lower switching losses and a more straightforward driving circuit than their predecessors, power bipolar junction transistors. The DC-DC boost converter, that uses more diodes for voltage enhancing, benefits from the FET's decreased "on resistance" by replacing the output rectifying diodes with synchronous rectification. The many DC-DC boost converters are depicted on the following diagram:

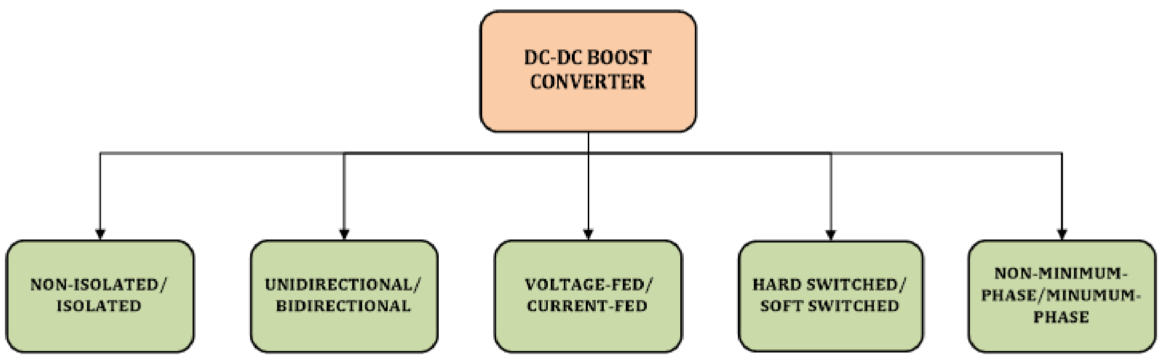

Fig. 1 - Classification of Step-up DC-DC Converter.

2.1. Isolated & Non-Isolated Step-up DC-DC Converter

Isolated DC-DC boost converter refers to a type of DC-DC boost converter that physically separates the DC input and the DC output. There are a number of situations in which an isolated DC-DC converter might be preferable than a non-isolated one.

- They cut off the connection between the input and the output at the ground.
- Due to its low output capacitance, numerous isolated DC-DC converters can be securely connected in series on the same DC bus.
- The DC voltage at the input can be "mapped" to the DC voltage at the output, even if the two values are very different.

It is possible to use either a linked inductor or a transformer to create a single- or two-stage, isolated dc- dc converter. Diagrams of single-stage and dual-stage isolated dc-dc converters are shown in Figure 2.

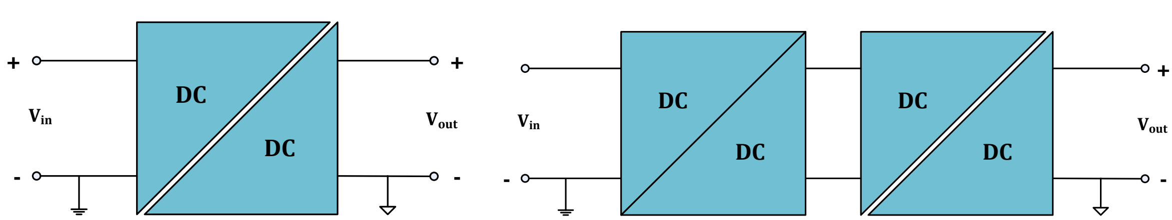

Fig. 2 - Single Stage& Two Stage Isolated DC-DC Converter

Isolated DC-DC boost converter refers to a DC-DC boost converter in which the DC input & DC output are coupled to the same potential. Non-isolated boost converters work by temporarily storing incoming energy in an inductor before discharging it into a capacitor at the device's output. The diagram below shows a non-isolated DC-DC converter in its most basic form.

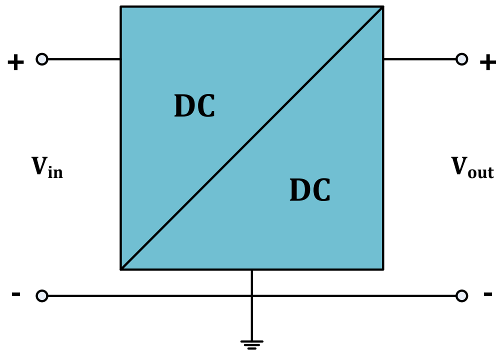

Fig. 3 - Common grounded Non-Isolated DC-DC Converter

2.2. Unidirectional and Bi-directional Step-up DC-DC Converter

Most basic DC-DC converters are used for one-way power transmission, where the input source serves solely to power the load (as in generation) or to soak up power from the output source (in regeneration). The schematics of a unidirectional and bidirectional DC-DC converter are shown in Figures 4 and 5, respectively.

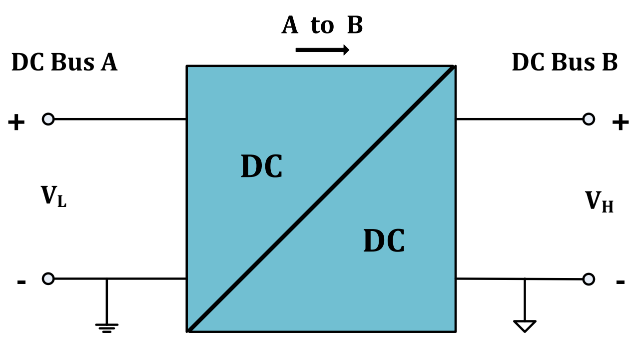

Fig. 4 - Unidirectional DC-DC Converter

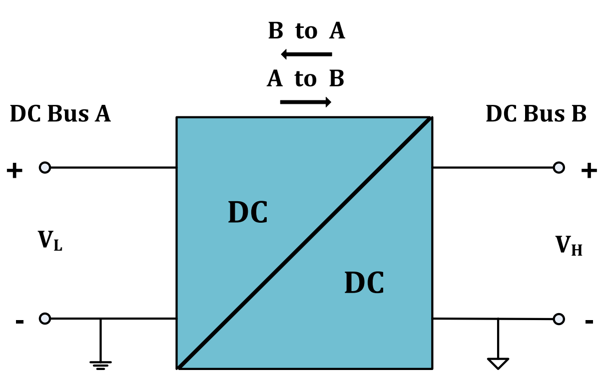

Fig. 5–Bi-directional DC-DC Converter

2.3. Voltage fed and Current fed Step-up DC-DC Converter

Depending on the input circuit, a DC-DC boost converter could be a voltage-fed converter or a current-fed converter. Figures 6 and 7 depict the designs of the two types of DC-DC converters. A voltage-fed dc-dc converter's input supply voltage is lowered by the capacitive input filter (Cin) before it is transformed to the output voltage. Power can be handled via the well-known voltage-fed full-bridge converter depicted in Fig. 6. The circuit's input is a capacitor, and its output is a low-pass filter.All DC-DC boost converters with switched-capacitor topologies, such as multilayer & flying capacitor converters, fall under the category of non-isolated voltage-fed dc-dc converters. These converters are typically designed for low-power applications because to their fast dynamic response. Input inductors are commonly used in the input circuit of current-fed dc-dc converters to boost the output voltage over the input voltage. Little-voltage applications of green energy, such as photovoltaics (PVs) and fuel cells, make extensive use of current-fed dc-dc converters because the input inductors can give a continuous input current, typically with low ripple.

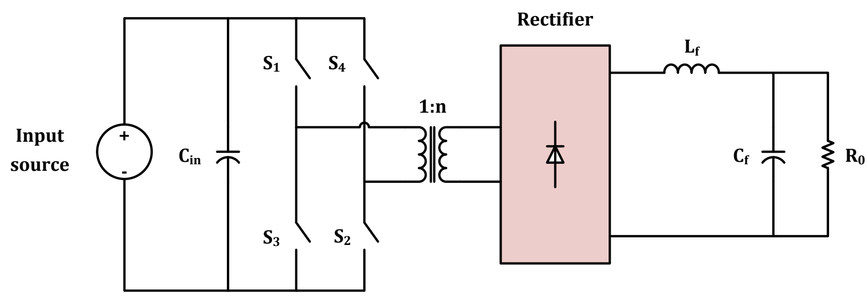

Fig. 6–Voltage-fed DC-DC Boost Converter

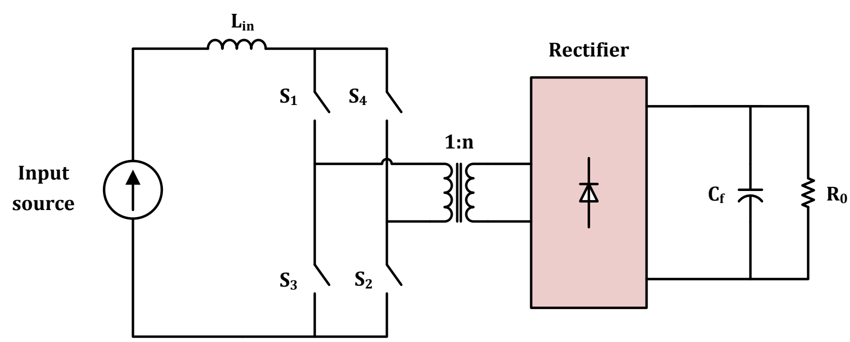

Fig. 7–Current-fed DC-DC Boost Converter

3. Controller Topologies

Choosing the right control scheme for bidirectional converters requires taking into account the architectures& control issues that arise in real-world applications. For uses that don't require isolation, a non-isolated configuration may be preferable because it doesn't call for a transformer, which can increase complexity and increase construction costs. Electrical separation, high reliability, the easy realisation of bidirectional flow of energy, soft-switching management, and shielding the equipment and operators for safety are only some of the many advantages of isolated topologies for high power applications. Because of the high frequencies at which transformers are generally utilised, these advantages are realised. While the choice of topology is important for bidirectional DC-DC converters, a unified and efficient control approach is also required. Different types of control for Bidirectional DC-DC converters are summarised in the following diagram.

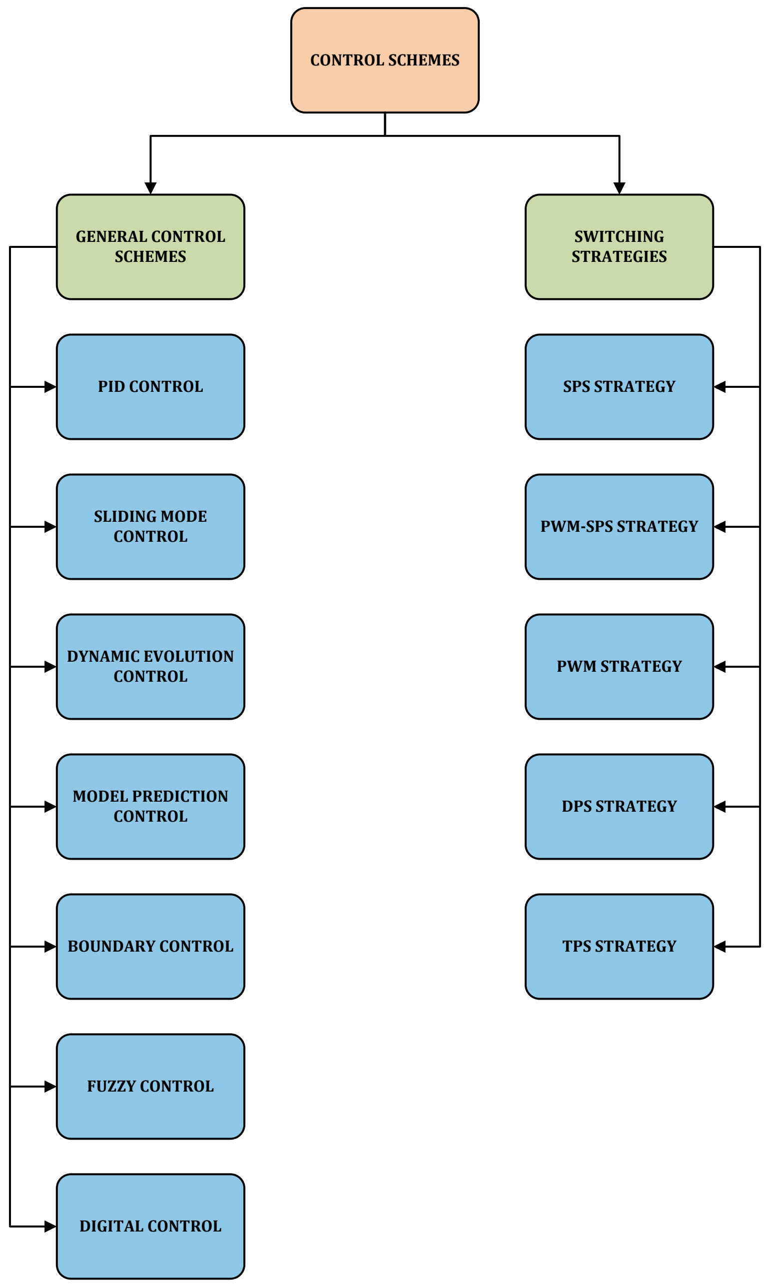

Fig. 8 – Classification of Control Strategies for Bi-Directional DC-DC Converter

3.1. Sliding Mode Control

Bidirectional DC-DC converters' dynamic equation is nonlinear because of nonlinear features in the converter's structure. Using the existing linearization method, a nonlinear system can be linearized around its equilibrium point, which can then be used as input to a control strategy. The diagram below illustrates the design of the proposed sliding mode controller.

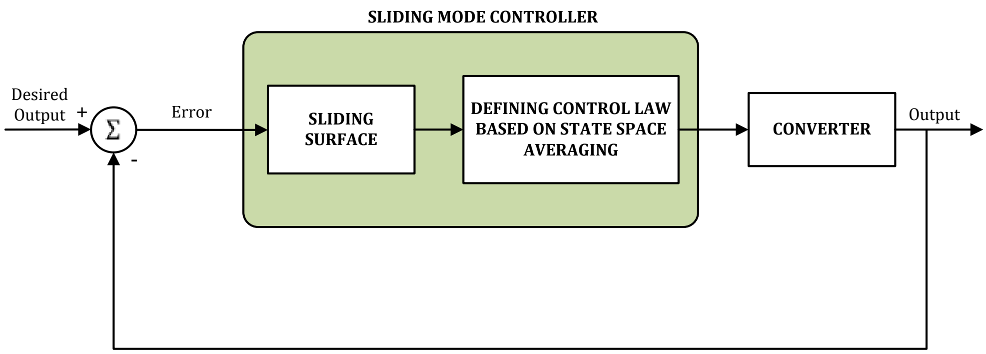

Fig. 9 – Structure of Proposed Sliding Mode Controller

Sliding mode control is a well-liked nonlinear control approach for both linear and non-linear systems due to its fast response time, stability against parameter fluctuations, and immunity to external disturbances. When a large-signal occurs in the bidirectional converter as a result of external perturbations, the regulator's behaviour cannot be predicted by the study of small-signal depending on the state space-averaging model.Sliding mode control is an appropriate control technique to address this challenge since it converges in finite time and is insensitive to external perturbations. However, this control approach is more difficult because precise parameters and state information are necessary.

4. Proposed System

4.1. Design and working of Converter

In order to increase the voltage between the input supply and the output load, a boost converter can be used. The step-up converter used in this study is depicted below in schematic form. A diode and a switch make up the converter's design. In this scenario, a MOSFET is being examined for use as a switch. The capacitance helps regulate and filter the voltage when a load resistance is attached across it.

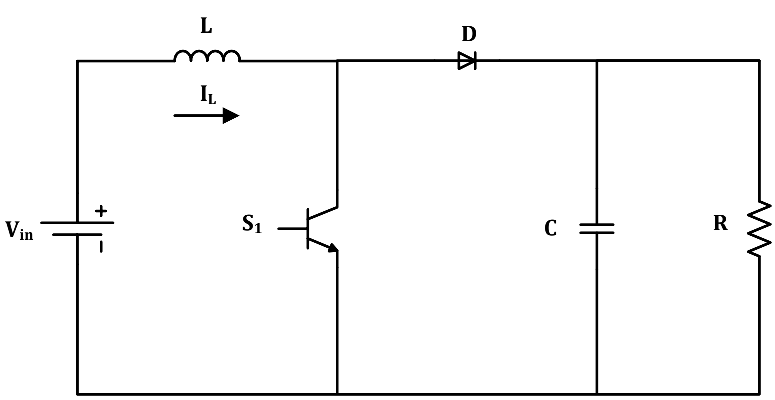

Fig. 10 – Schematics of boost converter

The converter has two modes of operation: one for when the MOSFET is on, and another for when it is off. When the MOSFET is activated, current flows from V_{in} (+ve) through L to S1 and back to V_{in} (-ve). All that energy will be stored in the inductor till later. When the switch is in its closed position, it creates a short circuit with reduced resistance. Thus, this is the route taken by the electric current. The inductor is "charged," or makes energy storage, during this process. Whenever the MOSFET is disabled, current is restricted to the outer loop. During this process, the inductor will release its stored energy. Ultimately, the input voltage and the lost energy will both circulate through the circuit. As a result, the load voltage will exceed the supply voltage. To get the proper output voltage after the boost in input voltage, the controller is still required to regulate the converter's functioning. This article presents the controller design for this converter in depth.

4.2. Design of Controller

To develop an average state space model for this converter we require switch to operate in both closed mode and open mode of operation.
The State Space Equation is
$\dot{X} = \bar{A}x + \bar{B}u$
Where
$\dot{x} = A_1x + B_2u$ (Switch in closed position)
$\dot{x} = A_2x + B_2u$ (Switch in open position)
The Average State Space model is
$\dot{X} = \bar{A}x + \bar{B}u$
Where
$\bar{A} = A_1d + A_2 (1 - d)$
$\bar{B} = B_1d + B_2 (1 - d)$
d = Duty cycle
The above equations represent state space averaging
Closed mode of operation

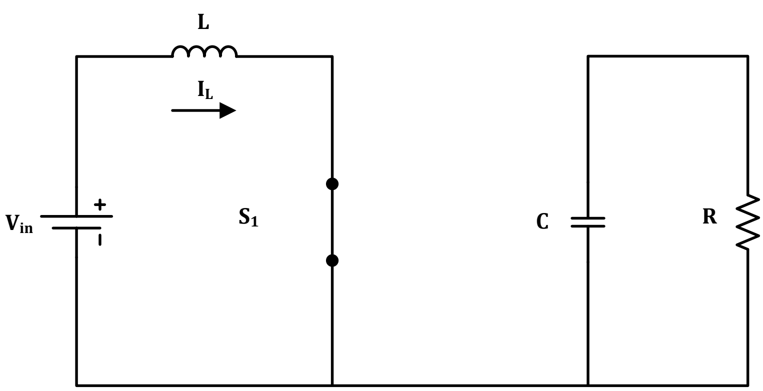

Fig. 11 – Closed mode operation of Boost Converter

The voltage across inductor is V_{in} as they are connected in parallel.

$$V_{in} = L\frac{di_L}{dt} \qquad (1)$$

Current through capacitor is current through load.

$$i_c = \frac{V_0}{R}$$

$$\frac{V_0}{R} = C\frac{dV_c}{dt} \qquad (2)$$

Consider state variables $x_1 = i_L$ and $x_2 = V_c$

$$\begin{bmatrix}\dot{x_1}\\ \dot{x_2}\end{bmatrix} = \begin{bmatrix}0 & 0\\ 0 & \frac{-1}{RC}\end{bmatrix}\begin{bmatrix}x_1\\ x_2\end{bmatrix} + \begin{bmatrix}\frac{1}{L}\\ 0\end{bmatrix} V_{in}$$

Open mode of operation

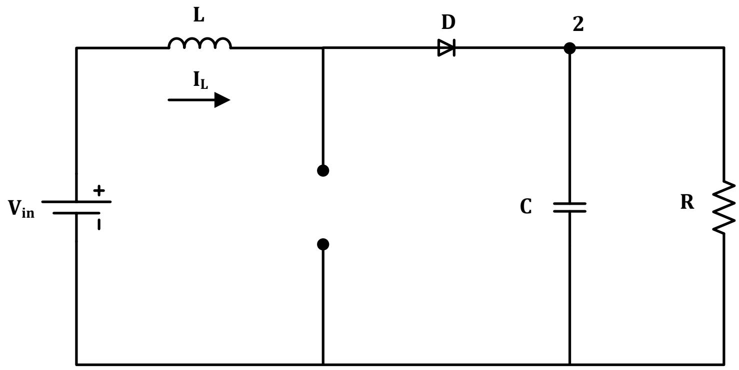

Fig. 12 – Open mode operation of Boost Converter

KVL to outer loop gives

$$-V_{in} + L\frac{di_L}{dt} + V_c = 0$$

$$L\frac{di_L}{dt} = V_{in} + V_c$$

KCL at node 2 gives

$$i_c + i_{out} = i_L$$

$$C\frac{dV_c}{dt} = i_L - \frac{V_c}{R}$$

Then,

$$\begin{bmatrix} \dot{x_1} \\ \dot{x_2} \end{bmatrix} = \begin{bmatrix} 0 & \frac{-1}{L} \\ \frac{1}{C} & \frac{-1}{RC} \end{bmatrix} \begin{bmatrix} x_1 \\ x_2 \end{bmatrix} + \begin{bmatrix} \frac{1}{L} \\ 0 \end{bmatrix} V_{in}$$

The average model by combining them will be

$$\dot{X} = \bar{A}x + \bar{B}u$$

$$\bar{A} = A_1 d + A_2\,(1-d)$$

$$\bar{B} = B_1 d + B_2\,(1-d)$$

The average model by combining them will be

$$\dot{X} = \bar{A}x + \bar{B}u$$

$$\bar{A} = A_1 d + A_2\,(1-d)$$

$$\bar{B} = B_1 d + B_2\,(1-d)$$

$$\begin{bmatrix} 0 & 0 \\ 0 & \frac{-d}{RC} \end{bmatrix} + \begin{bmatrix} 0 & \frac{-(1-d)}{L} \\ \frac{(1-d)}{C} & \frac{-(1-d)}{RC} \end{bmatrix}$$

$$\bar{A} = \begin{bmatrix} 0 & \frac{-(1-d)}{L} \\ \frac{(1-d)}{C} & \frac{-1}{RC} \end{bmatrix}$$

$$\bar{B} = \begin{bmatrix} \frac{1}{L} \\ 0 \end{bmatrix}$$

The average state space equation will be

$$\begin{bmatrix} \dot{x_1} \\ \dot{x_2} \end{bmatrix} = \begin{bmatrix} 0 & \frac{-(1-d)}{L} \\ \frac{(1-d)}{C} & \frac{-1}{RC} \end{bmatrix} \begin{bmatrix} x_1 \\ x_2 \end{bmatrix} + \begin{bmatrix} \frac{1}{L} \\ 0 \end{bmatrix} V_{in}$$

$$\dot{x_1} = -(1-u)\frac{x_2}{L} + \frac{V_{in}}{L}$$

$$\dot{x_2} = (1-u)\frac{x_1}{C} - \frac{1}{CR_0}x_2$$

Here the adaption for V_{in} and R so consider.

$$\theta = \frac{1}{R_0}$$

Then,

$$\dot{x_2} = (1-u)\frac{x_1}{C} - \frac{\theta}{C}x_2$$

Where u = controlled input to the converter is the duty ration function.

Estimation based adaption law design:

Here x_1 and x_2 are directly measured from circuit. So, the estimator is required for θ and V_{in}

So, the estimates of θ and V_{in} are $\hat{\theta}$ and $\widehat{V_{in}}$

Where $\hat{\theta} \rightarrow \frac{-1}{R_0}$

$\widehat{V_{in}} \rightarrow V_{in}$ Asymptotically

The estimator is

$$\dot{\widehat{x_1}} = -(1-u)\frac{\widehat{x_2}}{L} + \frac{\widehat{V_{in}}}{L} + K_1(x_1 - \widehat{x_1})$$

$$\dot{\widehat{x_2}} = (1-u)\frac{\widehat{x_1}}{C} - \frac{\hat{\theta}}{C}x_2 + K_2(x_2 - \widehat{x_2})$$

Here (K_1 and K_2) > 0 are observer gains

$\widehat{x_1}$ and $\widehat{x_2}$ are estimates of x_1 and x_2

Let us assume

$$\widetilde{x_1} = x_1 - \widehat{x_1}$$

$$\widetilde{x_2} = x_2 - \widehat{x_2}$$

$$\tilde{\theta} = \theta - \hat{\theta}$$

$$\widetilde{V_{in}} = V_{in} - \widehat{V_{in}}$$

From (1) and (2)

$$\left(\dot{x_1} - \dot{\widehat{x_1}}\right) = -(1-u)\left[\frac{x_2 - \hat{x}}{L}\right] + \frac{V_{in} - \widehat{V_{in}}}{L} - K_1(x_1 - \widehat{x_1})$$

$$\left(\dot{x_2} - \dot{\widehat{x_2}}\right) = (1-u)\left[\frac{x_1 - \widehat{x_1}}{C}\right] - \left[\frac{\theta - \hat{\theta}}{C}\right]x_2 - K_2(x_2 - \widehat{x_2})$$

By solving above equations

$$\dot{\widetilde{x_1}} = -(1-u)\left[\frac{\widetilde{x_2}}{L}\right] + \frac{\widetilde{V_{in}}}{L} - K_1\widetilde{x_1}$$

$$\dot{\widetilde{x_2}} = (1-u)\left[\frac{\widetilde{x_1}}{C}\right] + \frac{\tilde{\theta}}{C}x_2 - K_2\widetilde{x_2}$$

((3))

Now consider the quadratic Lyapunov function

$$V = \frac{1}{2}L\widetilde{x_1}^2 + \frac{1}{2}C\widetilde{x_2}^2 + \frac{1}{2y_1}\tilde{\theta}^2 + \frac{1}{2y_2}\widetilde{V_{in}}^2 \qquad (4)$$

Where,

$y_1 > 0$ and $y_2 > 0$ are design parameters

Time derivation of (4) gives

$$\dot{V} = -K_1L\widetilde{x_1}^2 - K_2C\widetilde{x_2}^2 - \tilde{\theta}\left[x_2\widetilde{x_2} + \frac{1}{y_1}\dot{\hat{\theta}}\right] + \widetilde{V_{in}}\left[\widetilde{x_1} - \frac{1}{y_2}\dot{\widehat{V_{in}}}\right] \qquad (5)$$

From the adaptation laws

$\tilde{\theta}$ and $\widetilde{V_{in}}$ terms must be cancelled. So

$$x_2\widetilde{x_2} + \frac{1}{y_1}\dot{\hat{\theta}} = 0$$

$$\dot{\hat{\theta}} = -y_1 x_2 \overline{x_2} \qquad (6)$$

$$V_{in} = y_2 \overline{x_1} \qquad (7)$$

Put 6&7 in 5 we get

$$\dot{V} = -K_1 L \overline{x_1}^2 - K_2 C \overline{x_2}^2$$

The switching surface will be

$$\sigma = \widehat{x_1} - \frac{Vref^2}{\widehat{Vin}} \hat{\theta}$$

V_{ref} is the desired output voltage

$$u_{eq} = 1 - \frac{\left(\widehat{V_{in}} + K_1 L \widehat{x_1} + \frac{\gamma_1 L V_{ref}^2}{\widehat{V_{in}}} x_2 \widehat{x_2} + \frac{\gamma_2 L V_{ref}^2}{\widehat{V_{in}^2}} \hat{\theta} \widehat{x_1}\right)}{\widehat{x_2}}$$

4.3. MATLAB Model

The following figure shows the MATLAB simulation model of the converter with the controller.

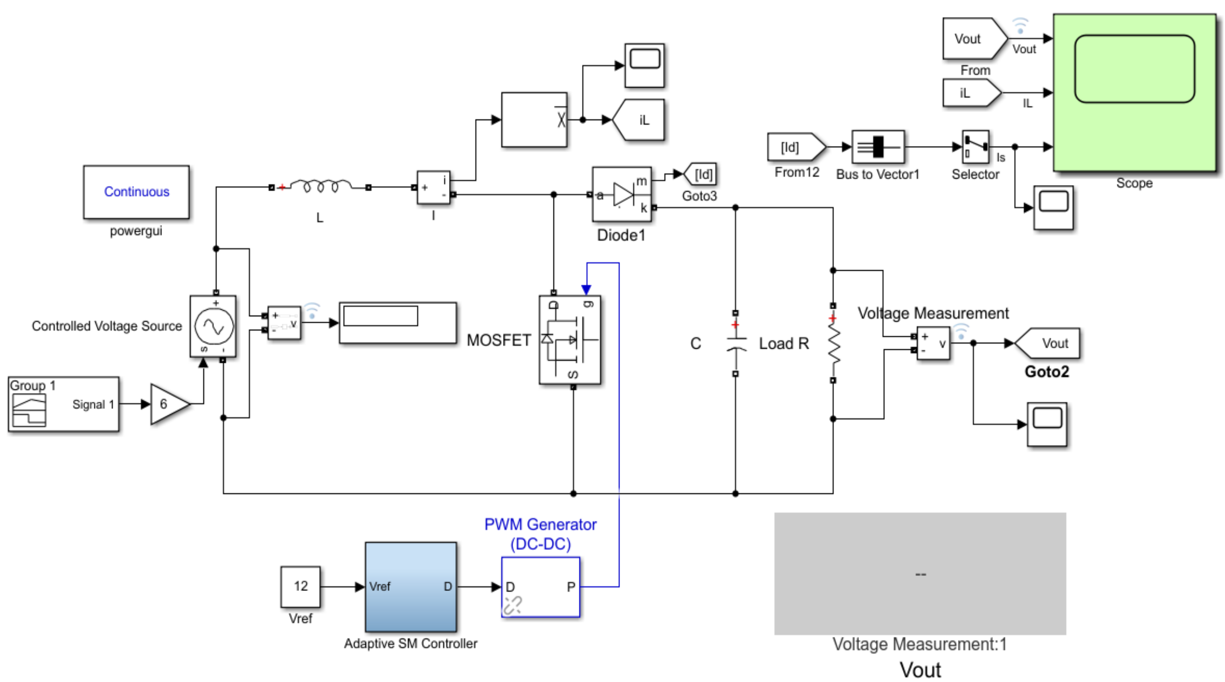

Fig. 13 – Simulation model of proposed controller with converter

4.4. Results

The following figures represents the results after simulating the above simulation model in MATLAB.

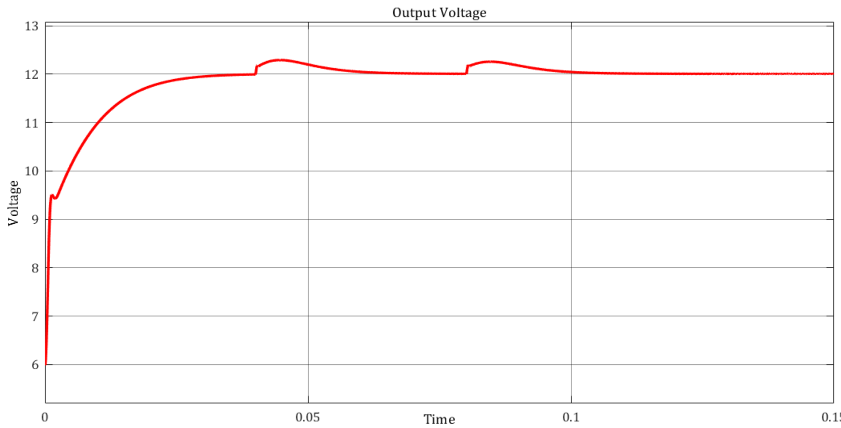

Fig. 14 – Output voltage Vs Time

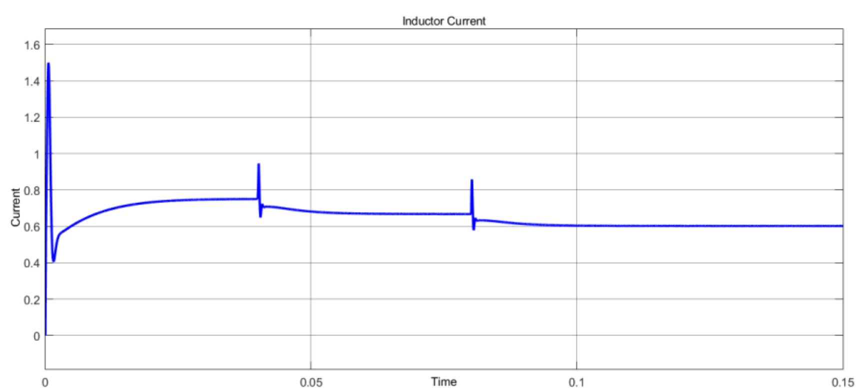

Fig. 15 – Inductor Current Vs Time

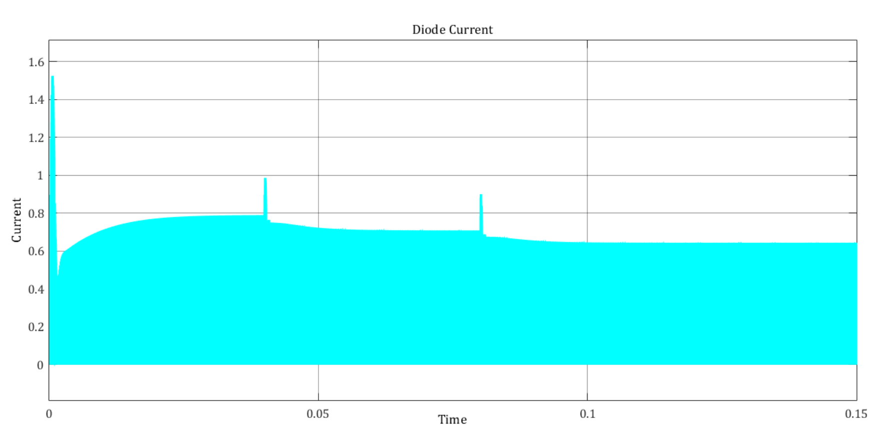

Fig. 16 – Diode Current Vs Time

5. Conclusion

An adaptive sliding mode control has been created for the boost converter to account for load resistance and input voltage fluctuations. A state of asymptotic stability for the closed-loop system is ensured. The boost converter was developed to be powered by a regulated voltage source whose output can be adjusted at regular intervals. The adaptive sliding mode controller is developed for such a boost converter with undetermined load resistance. The boost converter's MOSFET will be driven by pulses produced by the controller. As a result, the converter may now function in a closed-loop system. The controller takes the output of the converter as input and then supplies the MOSFET with pulses. By doing so, the desired voltage can be generated by the converter. In addition, the controller ensures that the converter maintains a constant output voltage and current regardless of changes in the input voltage or the load's resistance. The experimental outcomes show that the suggested adaptive SMC is very resilient and has great recovery properties to rapid input variations and unmodeled load variations. Both buck & buck-boost converters can benefit from the controller architecture.

References

[1] S. Oucheriah, L. G.-I. T. on industrial, and undefined 2012, "PWM-based adaptive sliding-mode control for boost DC–DC converters," ieeexplore.ieee.org, Accessed: Oct. 17, 2022. [Online]. Available: https://ieeexplore.ieee.org/abstract/document/6213544/?casa_token=tsDg7GgjecIAAAAA:OTiGkXtT0raxpUoR4WPA4lpSt-5mVANmkSCum86QfHjUBAf664d8059bS_2VABzzyKrXQFQacm9qPg

[2] M. S. M. Sarif, T. X. Pei, and A. Z. Annuar, "Modeling, design and control of bidirectional DC-DC converter using state-space average model," in ISCAIE 2018 - 2018 IEEE Symposium on Computer Applications and Industrial Electronics, 2018. doi: 10.1109/ISCAIE.2018.8405509.

[3] L. Shen, D. D. C. Lu, and C. Li, "Adaptive sliding mode control method for DC-DC converters," IET Power Electronics, vol. 8, no. 9, 2015, doi: 10.1049/iet-pel.2014.0979.

[4] H. Guldemir, "Sliding Mode Control of Dc-Dc Boost Converter," Journal of Applied Sciences, vol. 5, no. 3, 2005, doi: 10.3923/jas.2005.588.592.

[5] P. Singh and S. Purwar, "Sliding mode controller for PWM based Buck-Boost DC/DC converter as state space averaging method in continuous conduction mode," in ICPCES 2012 - 2012 2nd International Conference on Power, Control and Embedded Systems, 2012. doi: 10.1109/ICPCES.2012.6508100.

[6] Y. M. Alsmadi, V. Utkin, M. A. Haj-ahmed, and L. Xu, "Sliding mode control of power converters: DC/DC converters," Int J Control, vol. 91, no. 11, 2018, doi: 10.1080/00207179.2017.1306112.

[7] B. Taheri, M. Sedaghat, M. A. Bagherpour, and P. Farhadi, "A New Controller for DC-DC Converters Based on Sliding Mode Control Techniques," Journal of Control, Automation and Electrical Systems, vol. 30, no. 1, 2019, doi: 10.1007/s40313-018-00427-w.

[8] A. S. L. V. Tummala, R. Inapakurthi, and P. v. Ramanarao, "Observer based sliding mode frequency control for multi-machine power systems with high renewable energy," Journal of Modern Power Systems and Clean Energy, vol. 6, no. 3, 2018, doi: 10.1007/s40565-017-0363-3.

[9] T. S. L. V. Ayyarao, "Modified vector controlled DFIG wind energy system based on barrier function adaptive sliding mode control," Protection and Control of Modern Power Systems, vol. 4, no. 1, 2019, doi: 10.1186/s41601-019-0119-3.